Supporting Online Material for

# Self-Organized Spatial Patterns of Carbonate Formed via a Nonclassical Crystallization Pathway

Yiping Su,[a] Mingfang Cui,[a] Jianhua Zhu,*[ab] Yali Li,[a] Jufen Yan[a]

[a]Anhui Province Key Laboratory of Metallurgical Emission Reduction & Resources, Anhui University of Technology, Hudong Street 59, Maanshan, Anhui, China. 243002.

[b]Metallurgical Reduction and Comprehensive Utilization of Resources of Key Laboratory of Ministry of Education, Anhui University of Technology, Hudong Street 59, Maanshan, Anhui, China. 243002. Fax: +86 0555-2311879. Phone: +86 0555-2311879.

## 1. Materials and Methods

$CaCl_2$ (99%), $SrCl_2{\cdot}6H_2O$ (99.5%) and ammonium carbonate were of analytical grade. They were bought from Shanghai Chemical Reagent Company and used as received without further purification. Poly(allylamine hydrochloride) ($[-CH_2CH(CH_2NH_2{\cdot}HCl)-]n$ , PAH, Mw=15 KDa) was purchased from Aldrich accompany. All glassware (glass bottle and small pieces of glass substrate) were cleaned and sonicated in ethanol for 5 min, after being rinsed with distilled water and further soaked with a $H_2O$-$HNO_3$ (65%)-$H_2O_2$ (1:1:1,V/V/V) solution, then rinsed with doubly distilled water, and finally dried in a constant temperature drying oven.

## 2. Crystallization Experiments

Crystallization experiment was performed by a gas diffusion procedure in the presence of PAH (22±1°C). A stock aqueous solution of $CaCl_2$ was freshly prepared in boiled doubly distilled water and bubbled with $N_2$ for 2 h before usage. Then 10mL $CaCl_2$ solution was added into a glass bottle containing different molar fractions of $SrCl_2$. The polymer in a desired quantity was added to the $CaCl_2$ solution whilst stirring. Small microscope coverslips were placed at the bottom of the bottles in a desiccator. Finally, three glass bottles (10 mL) of crushed ammonium carbonate were also covered with Parafilm, punched with three needle holes, and were put at the bottom of the desiccator. At a different time, the samples were recovered, briefly washed with pure water, and allowed to dry on the air.

## 3. Titration Experiments

The titration experiments were carried out according to literatures by Denis Gebauer et al.[1] At first, the 10 mM carbonate buffers were prepared using mixtures of sodium carbonate (10 mM) and sodium bicarbonate (10 mM) solutions to give desired pH values. All experiments were performed at 25±1℃ in a 50 mL beaker filled with 25 mL carbonate buffer (pH=9.7). 20 mM dilute calcium chloride solution was tuned to desired pH value before titration. Then it was added into an excess carbonate solution at a constant rate (15 μL/min) while recording the concentration of calcium ions by a $Ca^{2+}$-ion selective electrode (Mettler Toledo S220) automatically. Changes in pH were automatically back-titrated by automatic titrator (LeiCi ZDJ-5), so that the equilibrium changed between carbonate and hydrogen carbonate induced by pH could be avoided. To figure out the role that PAH played during the crystallization of calcium carbonate, the polymer was added into the carbonate buffer. In addition, we also introduced different doping ions into the calcium chlorine solution to clarify their impact on the crystallization mode. Electrodes, glass vessels were cleaned with 10% acetic acid and carefully rinsed with distilled water after every experiment.

## 4. Characterization

XRD patterns were obtained on a Japan Rigaku Ultima IV X-ray diffractometer equipped with graphite-monochromatized Cu-Kα radiation (λ=1.54178 Å). The proportion of different phases was calculated automatically by the Rigaku Data Analysis software PDXL 2.0. The SEM images were recorded on a field-emission scanning electron microscope (JEOL S4800, 5 kV). Energy-dispersive X-ray (EDX) spectroscopy measurements were carried out at 10 kV with the help of an installed Oxford INCA microanalysis system. FT-IR spectra were measured on a Nicolet 6700 FTIR spectrometer from 400 to 4000 cm$^{-1}$ at room temperature. The size distribution was characterized on a dynamic light scattering instrument (Dynapro-MS800 ATC, England). The optical microscopy and polarized optical microscopy (POM) images were taken with a Leica microscope (DM 6000, German). Precipitation was analyzed by using Raman microscopy (LabRAM HR800). Micro-Raman Raman measurements were carried out in a Renishaw 2000 Raman microscope using a 785 nm diode laser as the excitation source. The laser was focused onto the sample using a 50× (numerical aperture NA 0.75) objective, enabling the individual structure of the particles to be determined.

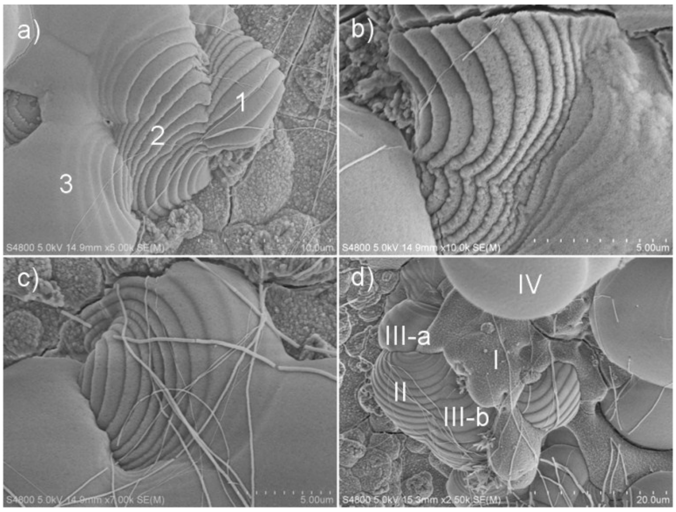

**Fig. S1** SEM images of structure patterns. a) Different adjacent concentric rings overlap one another. b) Two ring patterns developed at the same time merged into each other. (c) Later formed liquid precursor submerges the early pattern. d) Complex microstructures composed of patterns, coarse films and smooth globules.

Notes:

How do we judge the time sequence of different patterns? Firstly, the early formed pattern is often overlapped by the later one. As showed in Fig. S1a, Region 2 is partially covered by Region 3. But it also has overlapped Region 1. We are certain that Region 1 is the earliest pattern formed. Then Regions 2 develops, and finally Regions 3 grows. If the various patterns evolve at the same time, they will merge into each other and form new wavy patterns (Fig. S1b). Even in a single pattern, the time sequence still can be judged by the overlapping relationship. As showed in Fig. 1c, the smoothing edge has covered the ring pattern inside. It can be concluded that the smooth regions are formed before the ring pattern inside. Considering that the smoothing microstructures are part of ring pattern, we can judge that above pattern is initially developed from the centre of circle. That is, self-organized patterns are in facet evolved from their centers. Of course, the surface roughness of different structures can provided more useful clues about their growing course. As early formed structures will continuously grow via aging process, they usually show coarse surface. However, the later formed ones via liquid precursor maintain smoothing surface of droplets. Considering above two factors, we can predict the time sequence of complicated patterns (Fig. S1d).

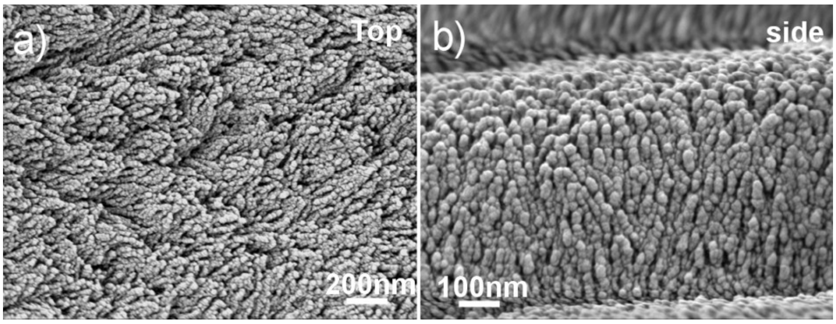

**Fig. S2** Magnified images of surface-relief structures. (a) Top view. (B) Side view.

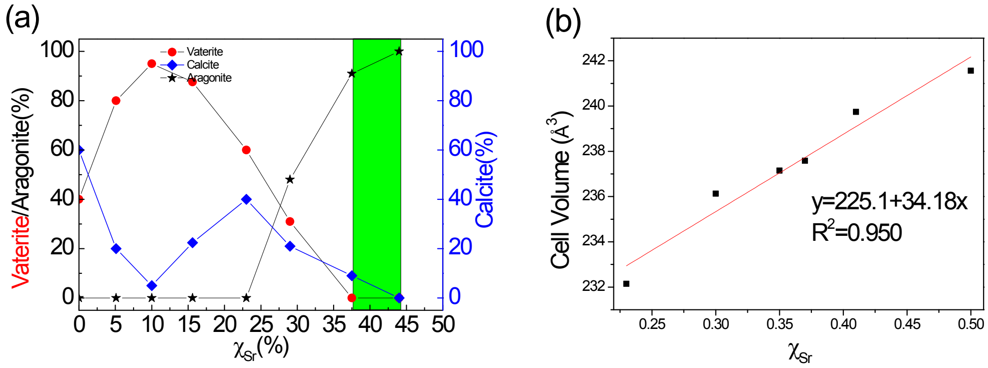

**Fig. S3** a) Percentage of different polymorphism vs $\chi_{Sr}$. Green region presents the experimental window for growth of carbonate patterns. Notes: Aragonite crystals come into being when $\chi_{Sr}$ increases to 23%. In the $\chi_{Sr}$ ranges between 37-44%, aragonite phase increase to 80-99%. b) Cell volumes of aragonitic $CaCO_3$ formed via a gas-diffusion process in the presence of PAH and at distinct $Sr^{2+}$ molar fractions in bulk solution. Values were derived by least-squares minimization of the XRD patterns. The cell volume increases linearly as the strontium ions are incorporated into the orthorhombic crystal system. Fits to the data give slopes of 34.18 ($Å^3/\chi_{Sr}$) ($R^2 = 0.950$) for $(Ca, Sr)CO_3$.

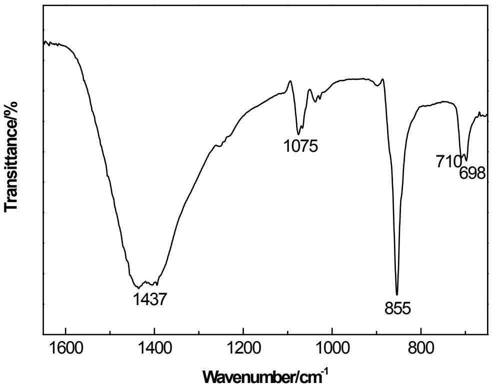

**Fig. S4** FT-IR spectrum of carbonate sample.

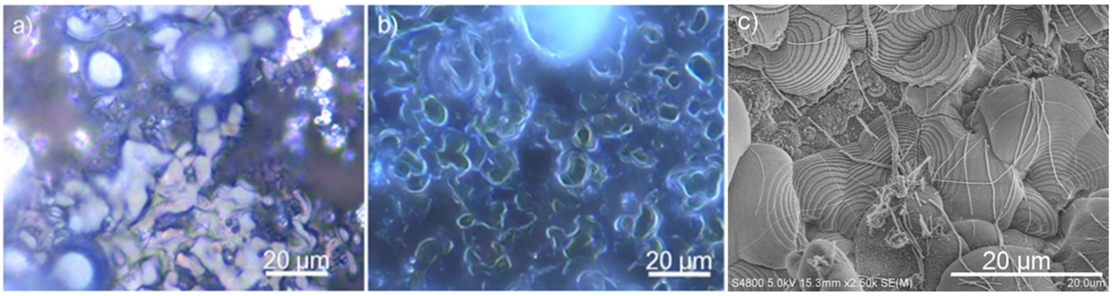

**Fig. S5** a) The optical micrograph of 3D motifs. b) The reflected polarized image. c) SEM image of 3D patterns.

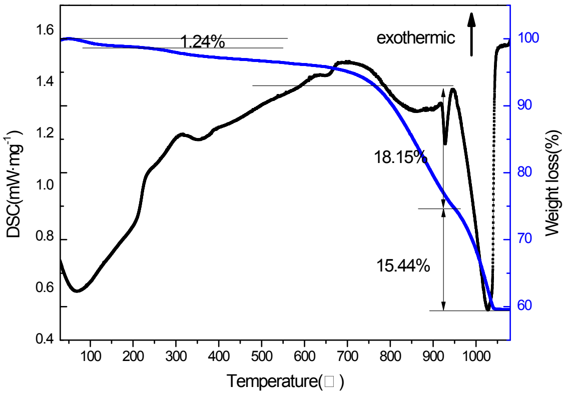

**Fig. S6** TG/DSC curves of 3D motifs.

Notes:

The first weight loss of 1.2% was complete up to 190°C, which corresponds to an endothermic peak in DSC curve due to dehydration. DSC curve showed two broad exothermic peaks at 190–350°C, which is contributable to the phase transformation from amorphous to crystalline carbonates as little weight loss can be observed. Obviously, the existence of amorphous phase indicates that self-organized carbonates were not completely crystallized and they may grow via solidification or partial crystallization process. The second weight loss ascribes to the degradation of PAH from 190°C to 762 °C. Characteristic decomposition of $CaCO_3$ (18.15 wt%) occurs at 762-950°C. and decomposition of $SrCO_3$ (15.44%) takes place at 950-1050°C. From above analysis, we can calculate that precipitation is composed of 41.25 wt% $CaCO_3$, 53.20 wt% $SrCO_3$, and about 4.31 wt % PAH.

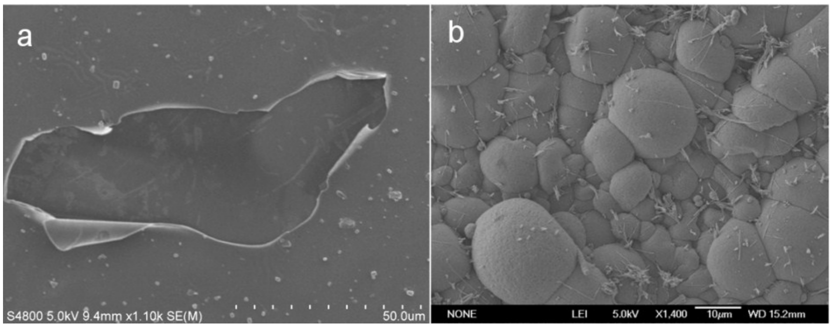

**Fig. S7** Mineral products obtained at different PAH concentrations with fixed $\chi_{Sr}$ of 0.38. (a) PAH=0.75g/L. (b) PAH=2.0 g/L.

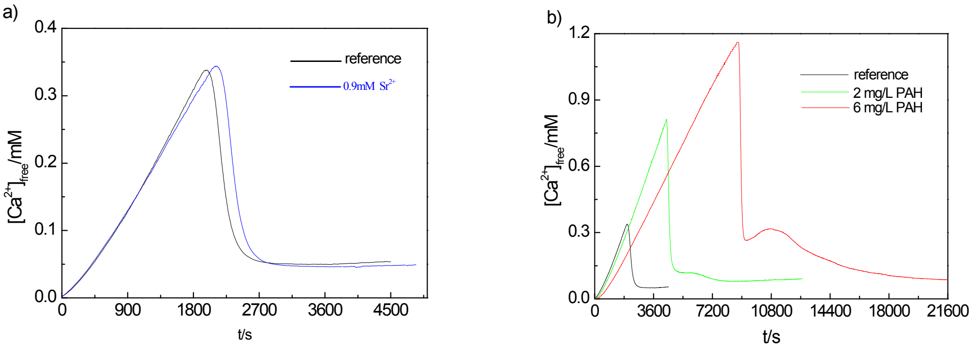

**Fig. S8** a) Development of free calcium concentration upon continuous addition of calcium and Sr solution into 10 mM carbonate buffer (pH 9.75). b) $[Ca^{2+}]_{free}$ vs time upon titration of $CaCl_2$ solution into carbonate buffer with different concentrations of PAH.

**Table S1** Nucleation time and lifetime of liquid intermediates. [PAH]=6mg/L, $[Ca^{2+}]$ = 20 mM.

| $C_{PAH}$(mg*L$^{-1}$) | $\chi_{Sr}$ | $[Sr^{2+}]$ / mM | Nucleation time (s) | Lifespan of liquid precursor(s) |
|---|---|---|---|---|
| 0 | reference | 0 | 2005 | * |
| 6 | 0 | 0 | 8744 | 8400 |
| 6 | 0.125 | 2.5 | 9110 | 9800 |
| 6 | 0.25 | 5.0 | 10960 | 9600 |
| 6 | 0.33 | 10 | 9924 | * |

Notes: The nucleation time was obtained from the drop of the free calcium concentration in the titrating curves. The lifespan of liquid precursor was calculated when the free calcium concentration drops to the lowest points after nucleation. Then the free calcium ions keep in a higher concentration than calcium amorphous carbonate. The lifespan of liquid precursor is estimated from the start point to the ending point (Fig. 3), where the free calcium concentrations are approaching the reference levels after nucleation.

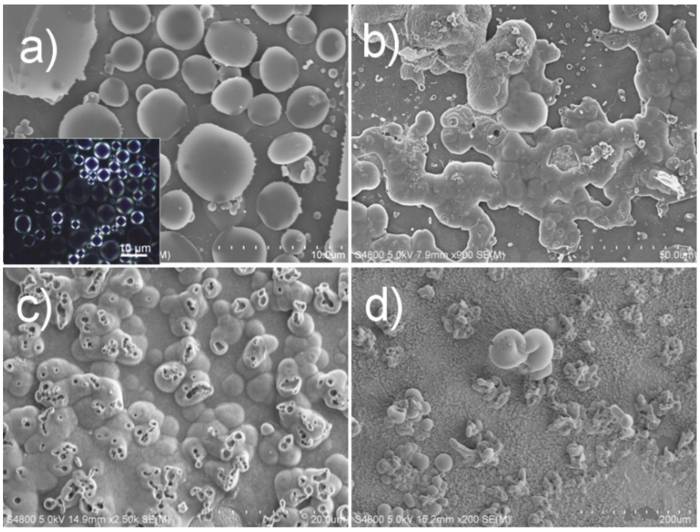

**Fig. S9** Early mineral intermediates in different growth stages. a) SEM image of liquid mineral precursor, inset is the polarized image. For 2 days. b-c) Gradual formation of mineral film. For 3 days. d) Growth of globules on mineral films. For 4 days. [PAH]=0.1 g/L, [$Ca^{2+}$] =10 mM and [$Sr^{2+}$] =4-6mM.

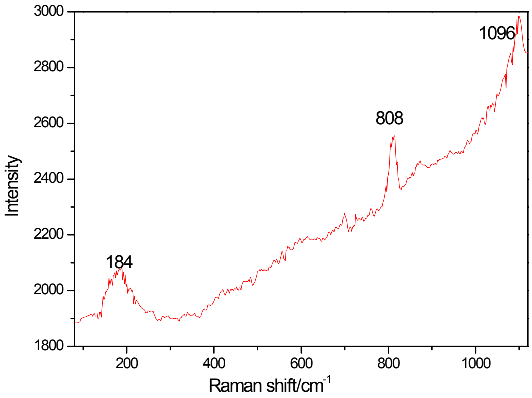

**Fig. S10** Micro-Raman of early formed globules obtained after 2 days.

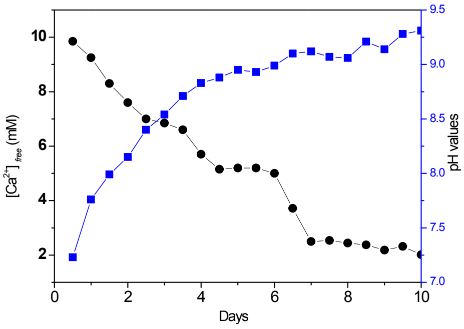

**Fig. S11** Concentration variations of calcium ions and changes of pH values during the mineralization.

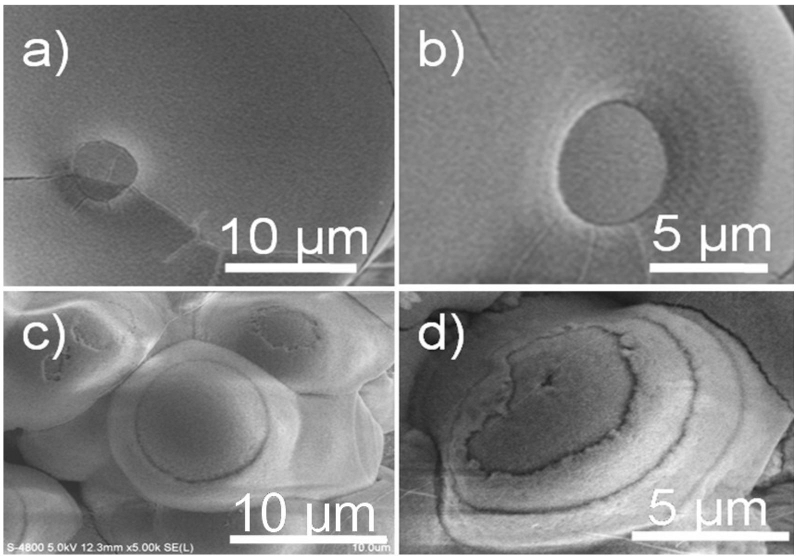

**Fig. S12** a-b) Early formed globules is almost immersed in the lately produced liquid precursor. 5 days; c-d) Globules surrounded by only one or several ring pattern. 7 days.

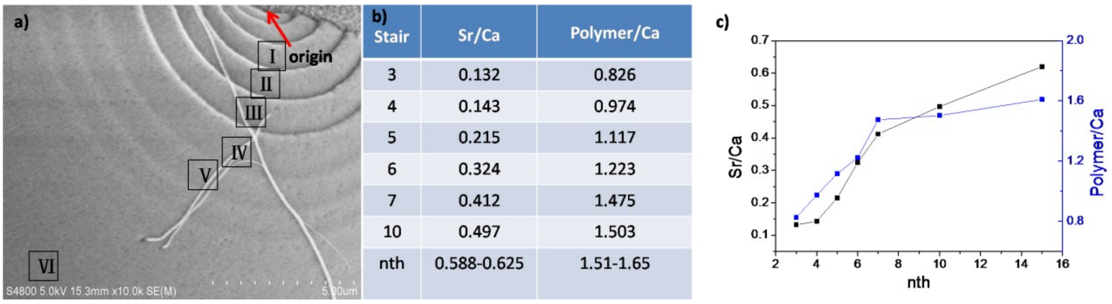

| Stair | Sr/Ca | Polymer/Ca |
|---|---|---|
| 3 | 0.132 | 0.826 |
| 4 | 0.143 | 0.974 |
| 5 | 0.215 | 1.117 |
| 6 | 0.324 | 1.223 |
| 7 | 0.412 | 1.475 |
| 10 | 0.497 | 1.503 |
| nth | 0.588-0.625 | 1.51-1.65 |

**Fig. S13** SEM-EDX analysis of 3D motifs. a) A ring pattern with deceasing height. I-VI show the micro-regions for EDX analysis. b) Table of Sr/Ca and Polymer/Ca. c) The graph of Sr/Ca and polymer/Ca in (a). Notes: In the pure carbonate, the ratio of C/Ca is 3. But ratios of C/Ca are evidently above 3 in our experiments owing to the introduction of polymer in crystallization process. Contents of polymer in above graphs refers to the surplus carbon (Polymer=C*total*-C*carbonate*). Nth refers to the smoothing globules without patterns.

1. D. Gebauer, A. Volkel and H. Cölfen, *Science*, 2008, **322**, 1819.